International Forum on Aeroelasticity and Structural Dynamics
IFASD 2017
25-28 June 2017, Como - Italy

Linearized Unsteady CFD for Gust Loads with TAU– IFASD 2017

Wolfgang Weigold[1], Bernd Stickan[1], Inocencio Travieso-Alvarez[2], Christoph Kaiser[3] and Patrick Teufel[1]

[1]Airbus Germany
Department of Gust and Aeroelastics
Wolfgang.Weigold@airbus.com
Bernd.Stickan@airbus.com
Patrick.Teufel@airbus.com

[2]Altran Deutschland SAS & Co KG
Aerospace Division
inocencio.travieso@altran.com

[3] DLR - German Aerospace Center
Institute of Aeroelasticity
Christoph.Kaiser@dlr.de

Keywords: gust, CFD

Abstract: For decades panel methods have been used in the industrial context to compute the unsteady aerodynamic model for gust load purposes. Additionally corrections with wind tunnel and/or steady CFD data have been applied to overcome the shortcomings of the panel methods, especially in the transonic regime. With the aim to compute a more realistic unsteady aerodynamic model without corrections, computational fluid dynamics (CFD) should replace the panel methods in the future.

Due to the large computational costs of CFD, an important enabler for the direct usage of unsteady CFD in the industrial context is linearized CFD. These codes allow computing harmonic motion and harmonic gusts directly in the frequency domain, preventing expansive unsteady computations in the time domain. See [2] and [3] for the here used TAU code and the included linearized frequency domain (LFD) solver from the German Aerospace Center (DLR).

In this research the complete aerodynamic model for the standard gust load process has been computed with TAU-LFD.

Tau-LFD provides frequency dependent aerodynamic data in half-generalized form, which can be introduced in a straightforward manner into the existing standard gust process.

1. INTRODUCTION

Gust loads computations for the complete flight domain involve the analysis of a huge amount of different combinations of gust direction, aircraft mass, altitude and airspeed. It is obvious that fast and robust methods are mandatory to achieve such a task in a reasonable timeframe. Assuming a linear behavior of the system allows for solutions in the frequency domain and re-use of existing solutions by superposition. Furthermore, the static 1-g flight loads can be calculated independently from the incremental gust loads. The total loads are then simply the sum of the two.

The equation of motion in modal coordinates for the gust problem reads

$$[-\omega^2 M_{hh} + i\omega B_{hh} - q_\infty\, Q_{hh}(M,k) + K_{hh}]u_h = q_\infty P_h^{gust} \tag{1}$$

with the generalized mass M_{hh}, damping B_{hh}, stiffness K_{hh} and aerodynamic response terms Q_{hh} on the left hand side and the generalized gust forcing P_h^{gust} on the right hand side.

This equation is solved for a unit harmonic gust input in the sampled frequency domain of interest. The result is a transfer function H for the generalized displacements u_h.

$$u_h(\omega) = [-\omega^2 M_{hh} + i\omega B_{hh} - q_\infty Q_{hh}(M,k) + K_{hh}]^{-1} q_\infty P_h^{gust} = H_{u_h}^{gust} \tag{2}$$

From this solution interesting quantities like displacements, accelerations and integrated loads can be derived using standard data recovery techniques.

As an example, the unit integrated loads on the structure are obtained using the force summation method, which results in a transfer function for the integrated loads P_{c1}

$$H_{P_{c_1}}^{gust} = T_{c1g}\left[\left(\omega^2 M_{gh} + q_\infty Q_{gh}\right)u_h + q_\infty P_g^{gust}\right] \tag{3}$$

where the subscript *gh* denotes half-generalize quantities. T_{c1g} is a matrix which relates forces and moments on the structural degrees of freedom g to integrated values on the output stations. Once these transfer functions have been computed, solutions for specific gust shapes or turbulence can be generated very quickly.

One of the most commonly used unsteady aerodynamic methods for gust loads computations is the doublet lattice method (DLM). In the DLM based process, the aerodynamic matrices for aircraft response and gust forcing in generalized and half-generalized form are calculated using the AIC matrix by simple matrix-vector multiplications. The AIC matrix Q_{jj} relates a local angle of attack (or downwash) w_j at each panel to a pressure coefficient. For a structural deformation the downwash w_{jh} is calculated from the modal panel deflection. The gust downwash w_j^{gust} represents the imposed harmonic wind distribution over the length of the aircraft. Matrix G_{gj} maps the aerodynamic forces to the structural degrees of freedom.

$$Q_{hh} = \phi_{gh}^T G_{gj} Q_{jj} w_{jh} = \phi_{gh}^T Q_{gh} \tag{4}$$

$$P_h^{gust} = \phi_{gh}^T G_{gj} Q_{jj} w_j^{gust} = \phi_{gh}^T P_g^{gust} \tag{5}$$

The theoretical results from the DLM method need to be adjusted to ensure that the real aircraft properties are accurately represented. One common technique, which is taken as a reference in this paper, is the factorization of the panel pressure coefficients by left multiplication of the AIC matrix with a weighting matrix W_{jj}:

$$Q_{jj}^{corr} = W_{jj} Q_{jj} \tag{6}$$

The weighting factors in matrix W_{jj} can e.g. be derived by comparing the load and moment distributions versus span with a set of selected reference values.

2. TAU-CFD

As the CFD solver, the DLR TAU-code is used to solve the steady and the unsteady Reynolds Averaged Navier Stokes (RANS) equations [4]. The solver works with a cell-vertex-based finite volume scheme on unstructured grids. For the following studies the Spalart-Allmaras model is used.

1.2 Time-Domain (TAU-TD)

To get the entries of the aerodynamic matrices Q_{gh} and P_g^{gust}, time-history data of harmonic time-domain computations are transferred with the Fast-Fourier Transformation to the frequency domain.

For this purpose the steady flow field is harmonically disturbed either by a structural eigenmode, a rigid-body mode or a gust velocity. The eigenmodes and rigid-body modes are transferred to the CFD mesh via CFD mesh deformation. The gust disturbances are modelled with the Disturbance Velocity Approach (DVA) (sometimes also called Field Velocity Approach), see [3]. The unsteady time-stepping in TAU is performed with the second order accurate dual time-stepping. Unsteady TAU results have been validated by many experiments, see [5,6].

1.3 Frequency-Domain (TAU-LFD)

The TAU-LFD method allows computing small amplitude, linear unsteady aerodynamics at very low costs. The reduction of computational costs is achieved by solving the aerodynamic equations directly in the frequency domain, using the assumption that an unsteady harmonic excitation leads to a harmonic aerodynamic answer. Details on the method can be found in [1]. Details on the expansion to gust modes and comparison and further validation can be found in [2] and [7].

3. VALIDATION OF TAU-LFD VERSUS TAU-TD

The aerodynamics inputs to the frequency domain gust computations are generated with the linearized CFD solver TAU. Although the method has already been validated, see for example [1] and [2], this exercise is repeated here for an industrial test case.

At first a comparison between a time-domain and a linearized computation is presented. Figure 1 shows the generalized air forces (GAF, Q_{hh}) for three different eigenmodes. Here the diagonal entries for different frequencies in Q_{hh} are plotted. The flight conditions for this comparison are Mach=0.86 and altitude 30,000 feet.

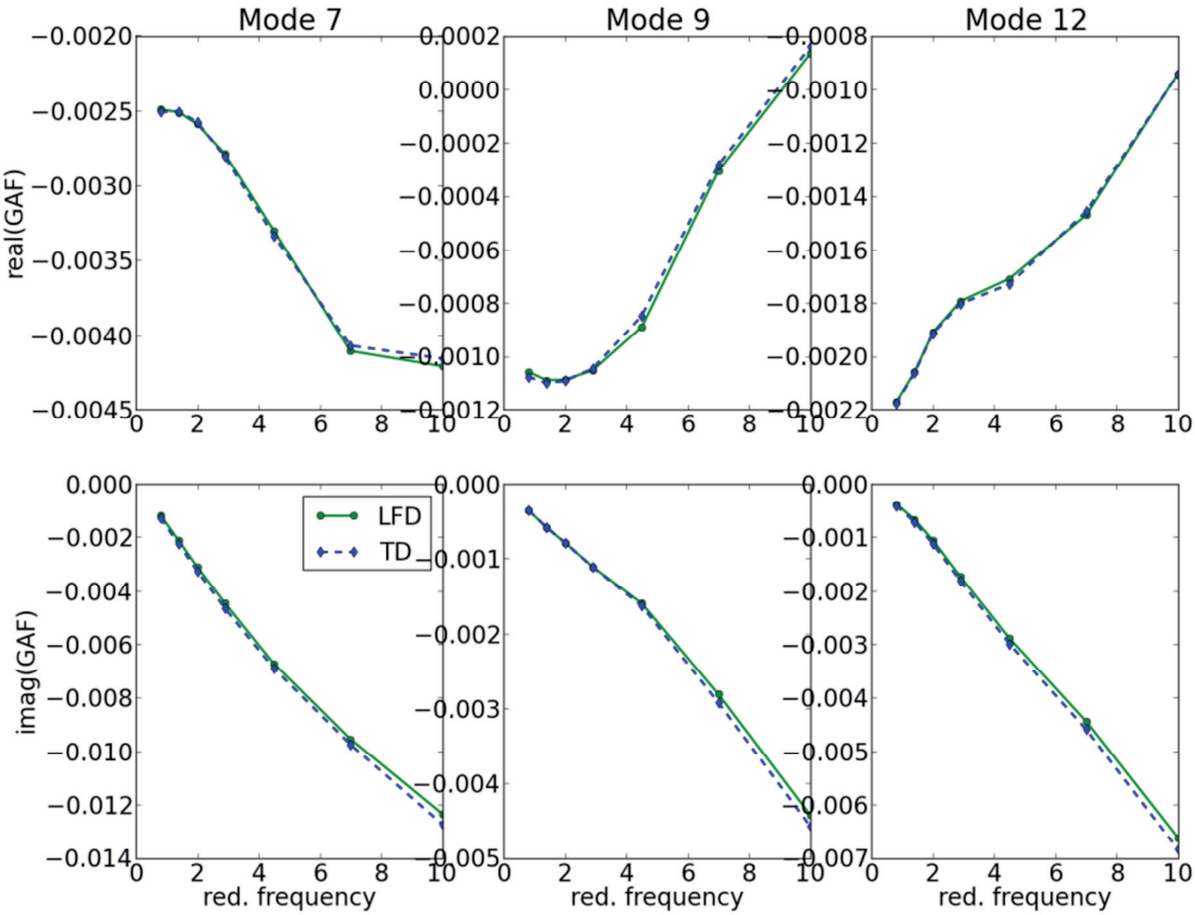

Figure 1: Comparison time-domain (TD) versus linearized (LFD) TAU : GAFs for 3 different flexible modes

The harmonic time domain computations have been performed with (only) 45 steps per period and a very small amplitude. The computation has been stopped when the phase of the GAF is converged to 0.1 degree accuracy. Depending on the frequency between 2.5 and 5 periods are needed to reach this target accuracy. In each time step the residuum is decreased by approximately 2 orders of magnitude.
The TAU-LFD computations did converge well with 60 GMRES vectors. The agreement between the simulation results is very good. Experience for more accurate time domain computations (more steps per period, etc.) show generally a convergence of the two methods.

Secondly a comparison of time-domain and linearized CFD is performed for a gust excitation. The harmonic time domain computations with very small vertical gust speed (0.01 m/s) have been performed with 50 steps per period. Again in each time steps the residuum has been converged by approx. 2 orders of magnitude. The simulation is stopped in this case if the phase of C-lift-influence of the gust is converged to 0.1 degree accuracy. As seen for the flexible mode, a good agreement can be achieved between the two methods.

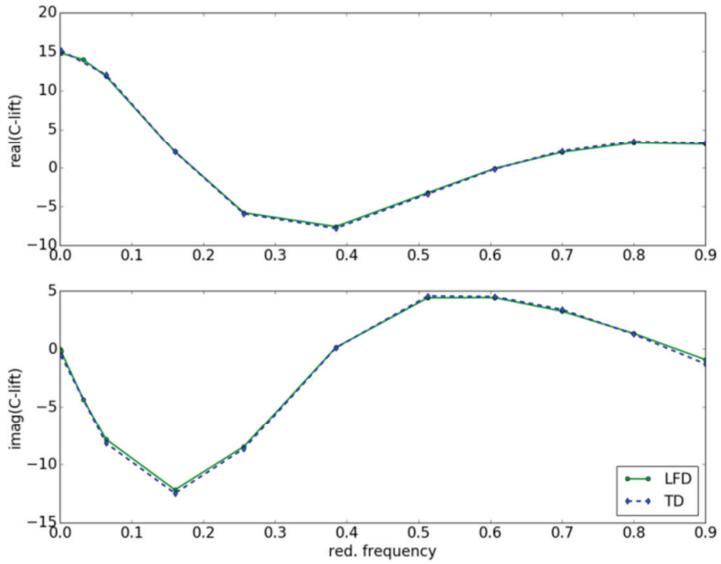

Figure 2: Comparison time-domain (TD) versus linearized (LFD) TAU: vertical gust influence on C-lift

Finally the solution for a vertical gust is validated against the rigid heave and pitch modes at a reduced frequency k=0.
Figure 3 illustrates this test setting. The plot shows that a rigid body rotation (Mode 5), a heaving velocity (Mode 3) and a vertical gust generate the same uniform angle of attack distribution along the aircraft. It is therefore expected that the aerodynamic response is also equal.

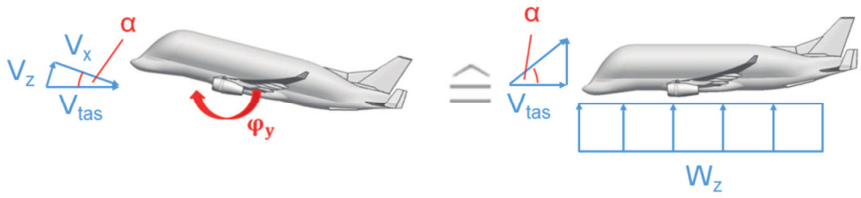

Figure 3: Similarity of pitch mode and vertical gust/heave velocity for frequency zero

Figure 4 shows the generalized lift amplitude and phase for a vertical gust mode in comparison to a heaving and pitching motion. All three results approach the same magnitude and the correct phase angle for $k \to 0$.

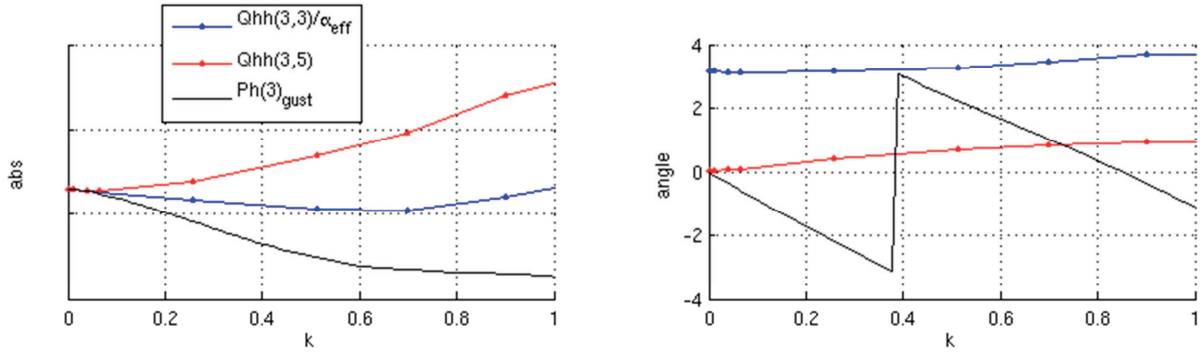

Figure 4: Comparison of generalized lift for heave (normalized with AoA), pitch and gust mode vs. reduced frequency

4. VALIDATION TAU-LFD VERSUS DLM

A low subsonic Mach number of 0.5 was chosen for validation of the process to ensure that the subsonic doublet lattice method could still be applied. The DLM model was adjusted using a simple scaling technique to match the shear force gradient due to a change in angle of attack from linearized CFD at zero frequency. A constant correction factor of 1.08 was applied to all wing panels, while the horizontal tail plane panels have been scaled by 0.9. This alone gives an almost perfect match for not only shear but also bending and torque on the wing, as shown in Figure 5, with differences well below 5%.

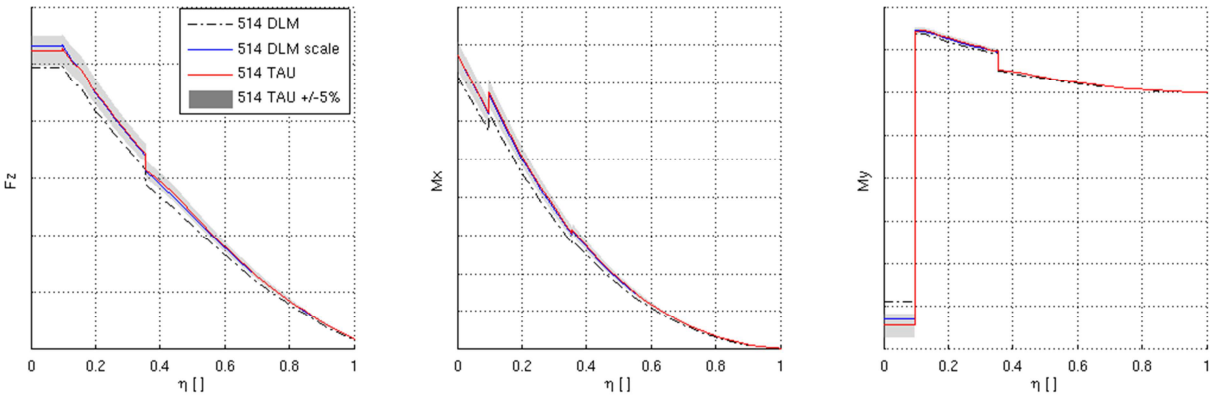

Figure 5: shear force, bending and torsion moment gradient due to AoA vs. span, DLM, adjusted DLM and CFD

Figure 6 shows a comparison of the wing loads versus span for the first elastic (wing bending) mode at a reduced frequency of zero. The differences between the adjusted DLM model and the CFD results are very small.

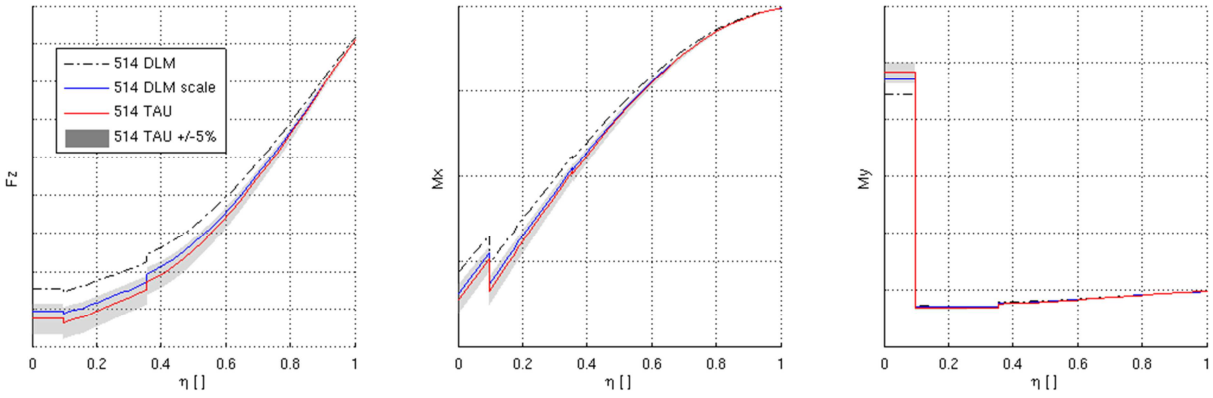

Figure 6: shear force, bending and torsion moment vs. span, mode 7

As a further validation, a steady elastic calculation for a constrained aircraft in modal coordinates is performed. The structural model is constrained for all 6 degrees of freedom at a single grid point in the center section of the wing. Then an aerodynamic load due to one radians angle of attack is applied and the elastic response is calculated. The equation reads

$$\begin{bmatrix} K_{hh} - q_\infty Q_{hh} & \phi_{gh_c}^T \\ \phi_{gh_c} & 0 \end{bmatrix} \begin{bmatrix} u_h \\ K_c \end{bmatrix} = \begin{bmatrix} P_h \\ 0 \end{bmatrix}, \quad P_h = q_\infty \phi_{gh}^T Q_{gh}(:,5) \tag{7}$$

where ϕ_{gh_c} denotes the modal matrix for the constrained degrees of freedom.

This equation is solved for the modal deflection u_h and the resulting grid point deflections u_g are calculated by multiplication with the modal matrix.

$$u_g = \phi_{gh} u_h \tag{8}$$

The resulting vertical deflection on the wing versus normalized wing span is shown in Figure 7. The solutions based on the CFD and the DLM aerodynamic models are almost identical.

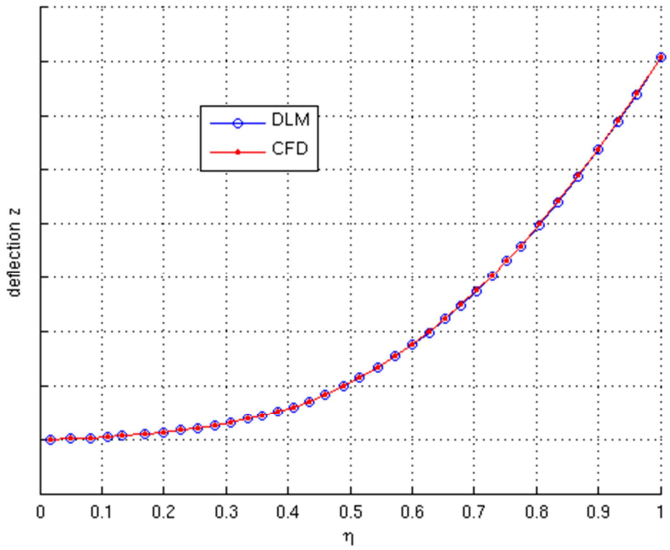

Figure 7: vertical deflection versus wing span

The next two figures show a comparison of the A/C lift force due to a heaving motion $Q_{hh}(3,3)$ and the pitching moment due to a pitch rotation $Q_{hh}(5,5)$ versus reduced frequency. Both methods agree very well, especially for the low frequency region. Results for the first elastic mode $Q_{hh}(7,7)$ are shown in Figure 10.

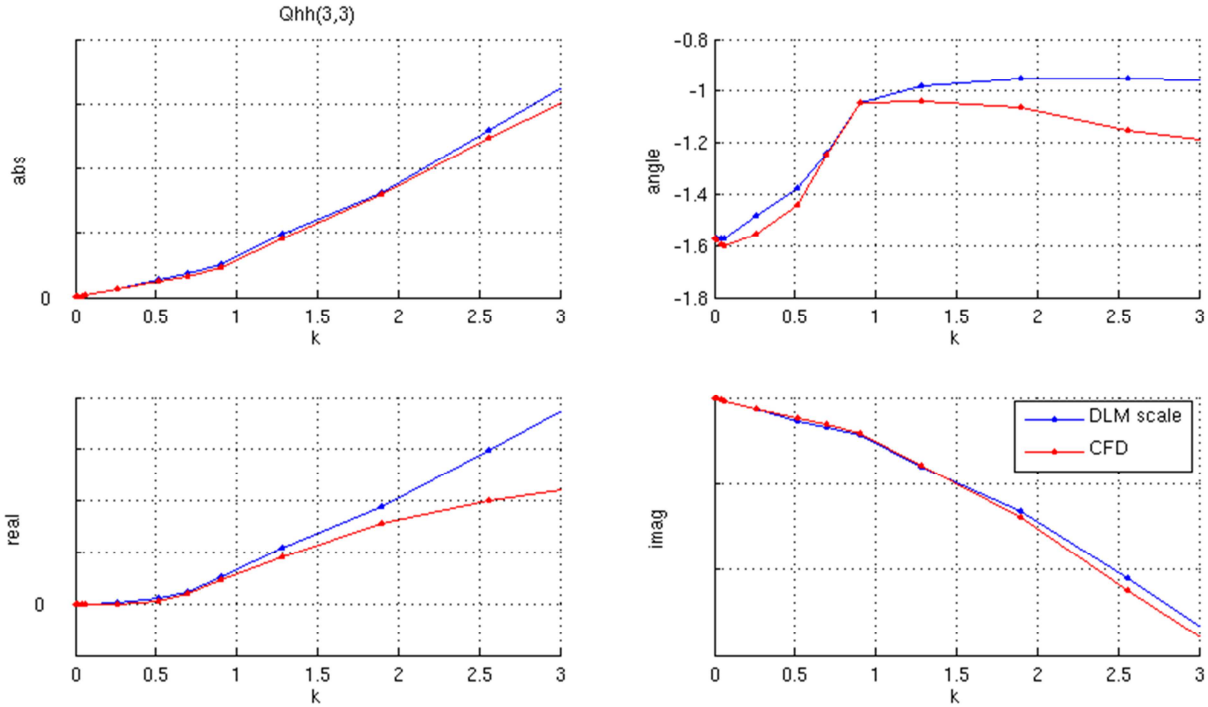

Figure 8: generalized aerodynamic force vs. reduced frequency, Mode 3

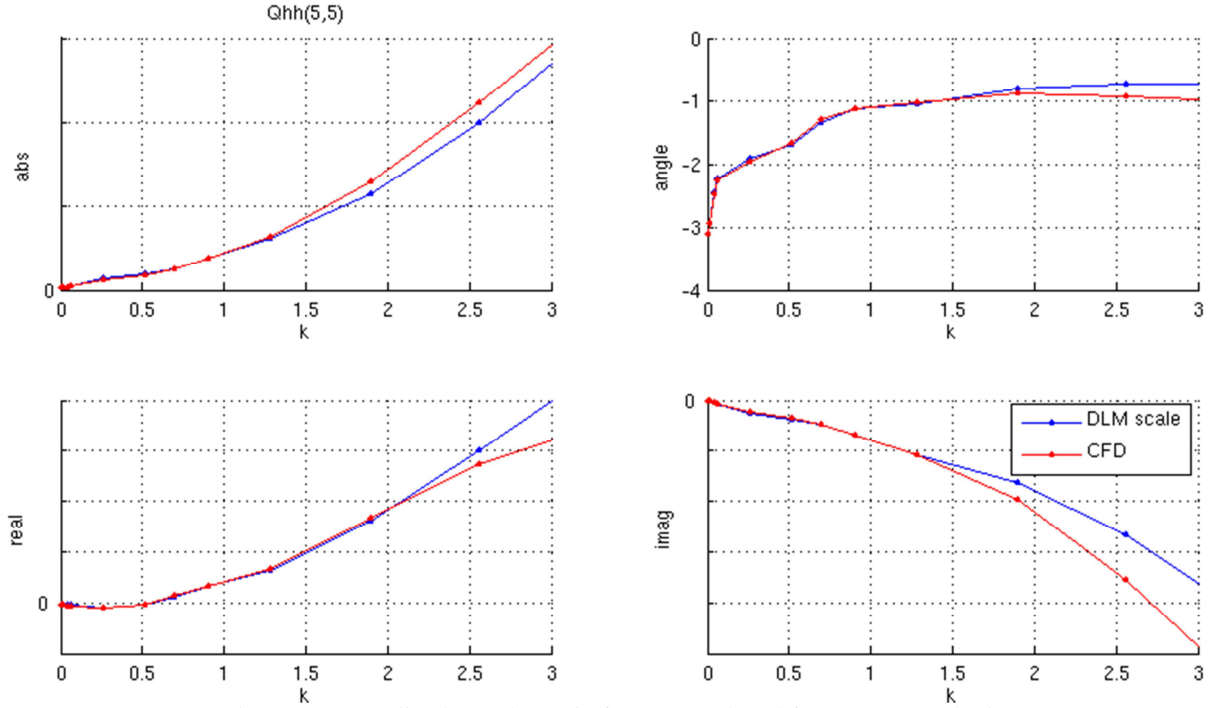

Figure 9: generalized aerodynamic force vs. reduced frequency, Mode 5

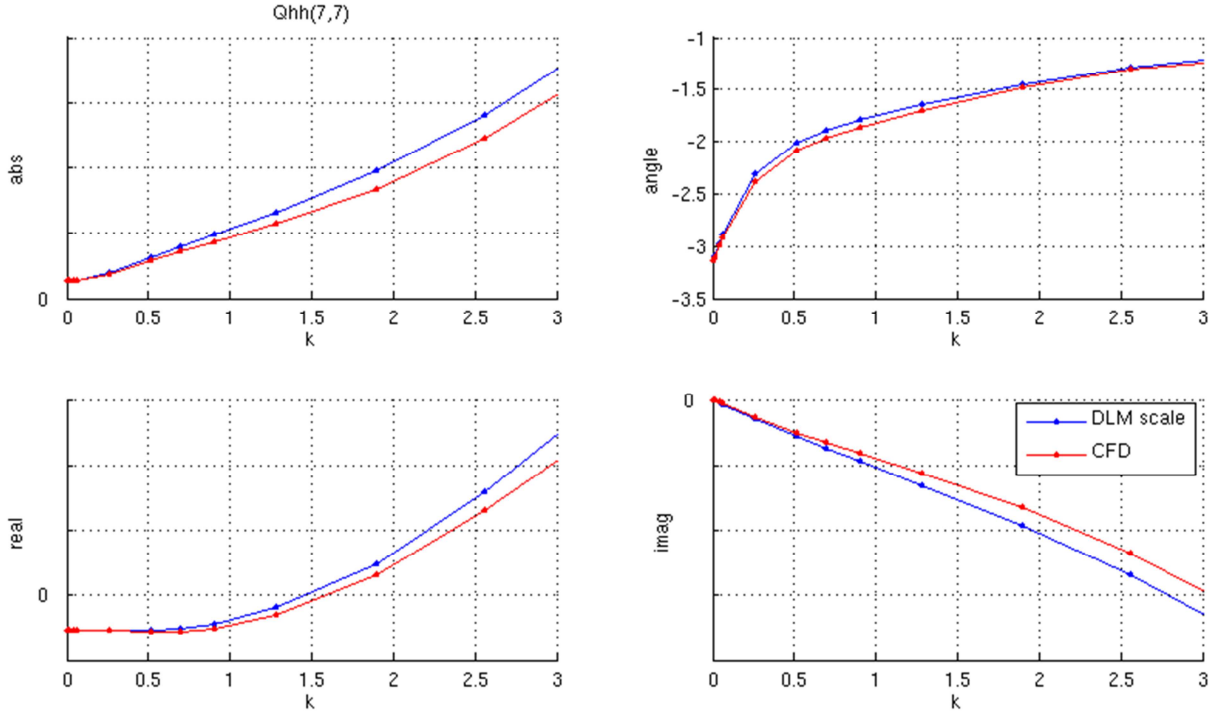

Figure 10: generalized aerodynamic force vs. reduced frequency, Mode 7

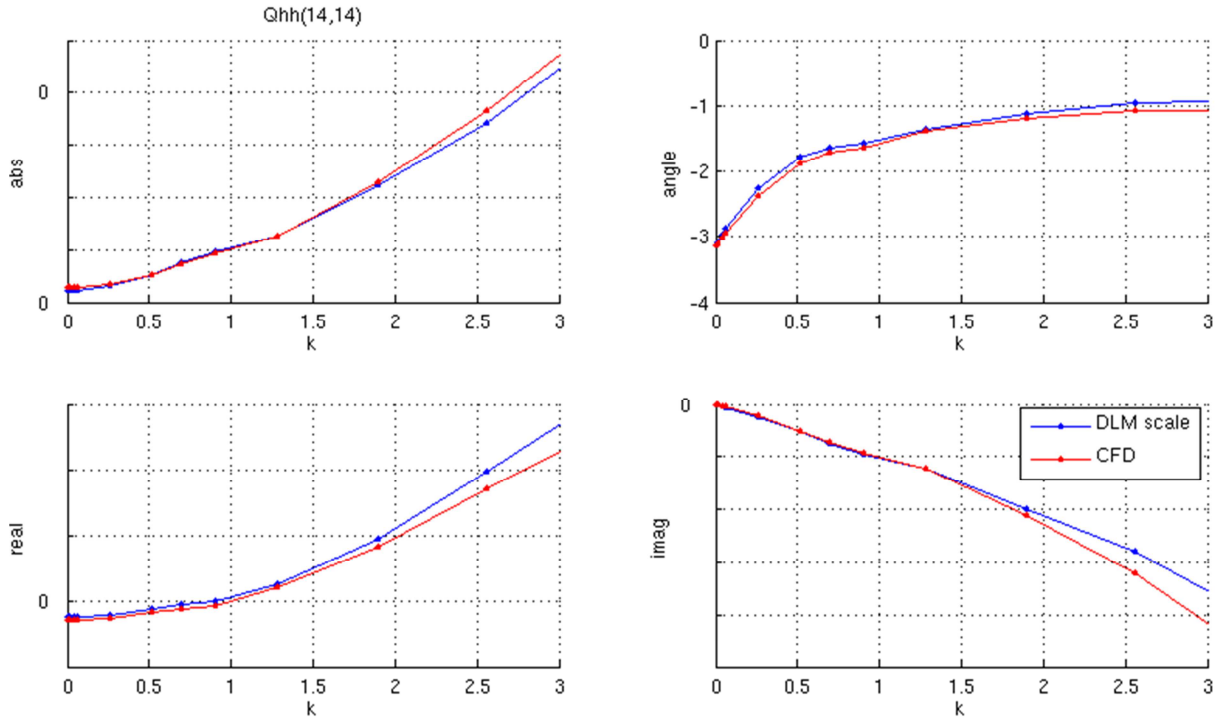

Figure 11: generalized aerodynamic force vs. reduced frequency, Mode 14

Finally, a comparison for the wing root bending moment due to a harmonic vertical gust versus reduced frequency is shown in the figure below. Again, both methods agree very well.

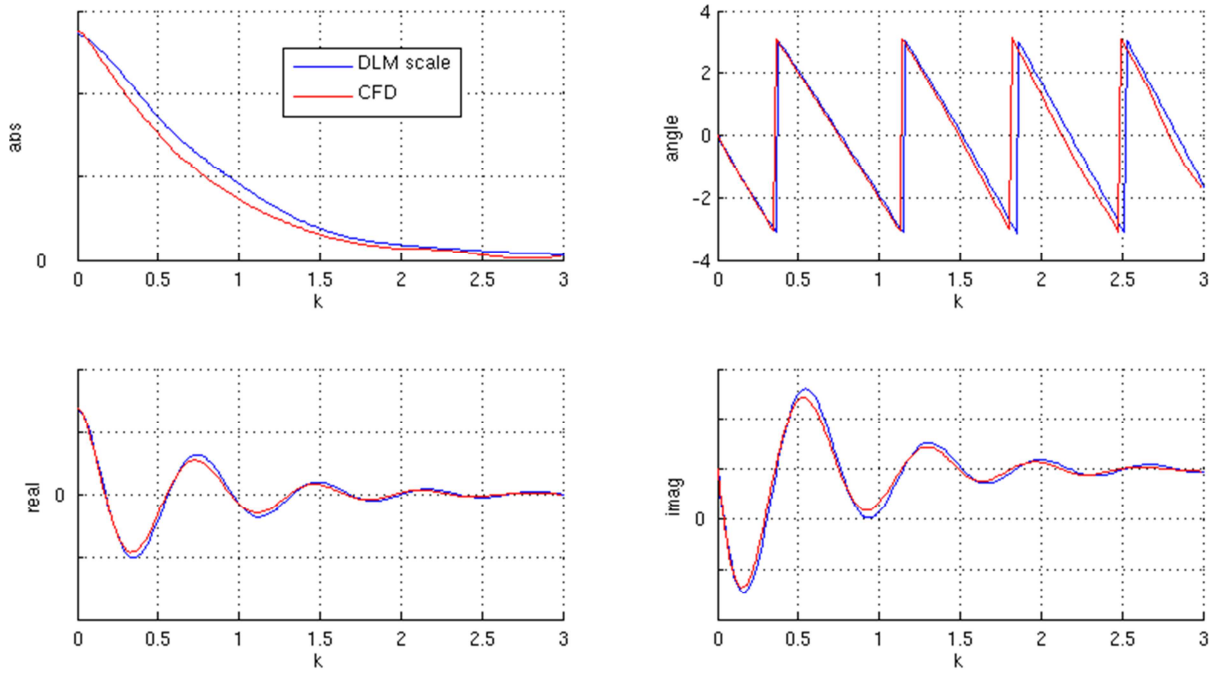

Figure 12: wing root bending moment due to vertical gust vs. reduced frequency

5. INTEGRATION OF TAU DATA IN GUST PROCESS

For a typical gust analysis, transfer functions are normally calculated for up to 1024 frequencies. It is obvious that performing CFD as well as DLM calculations for such a huge number of cases is not feasible. Therefore aerodynamic matrices are generated for a limited number of reduced frequencies only. These are clustered in the important low frequency region. Intermediate values are then calculated by interpolation.

Interpolation of half-generalized aerodynamic matrices due to modal deflection Qg1h is in general a straightforward task, as these are very smooth with respect to frequency. The situation is different for the gust modes, as these tend to show an oscillatory behavior versus frequency, see Figure 12. This is a direct outcome of the applied sinusoidal gust velocity which naturally inherits time delays.

A simple interpolation of real and imaginary parts does not give satisfactory results. To circumvent this problem an interpolation of the amplitude and phase is used instead. As the phase angles are not unique and may be shifted by multiples of 2 pi, phase unwrapping has to be applied to the data, as shown in Figure 13.

The resulting smooth curves can now easily be interpolated.

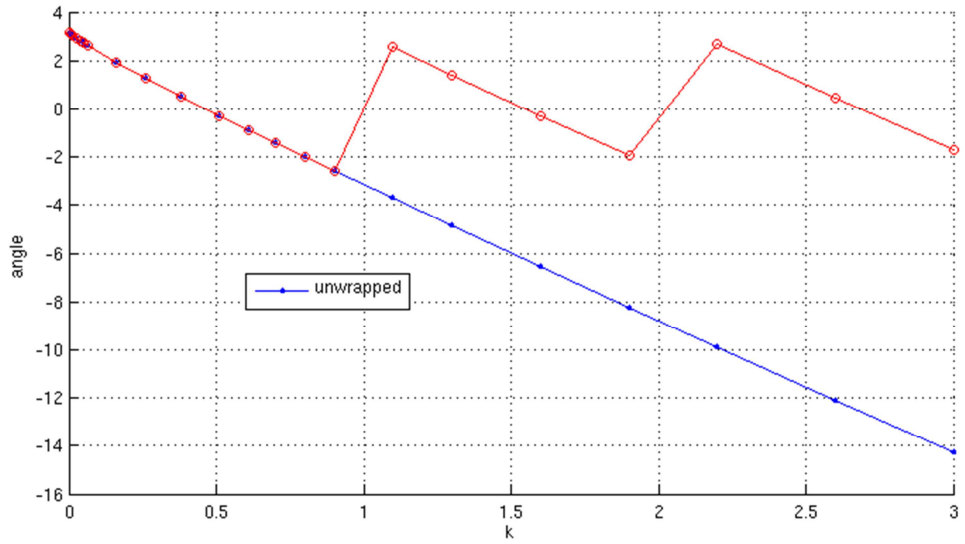

Figure 13: effect of phase unwrapping for an element of the gust force matrix $\boldsymbol{P_g^{gust}}$

This approach has been validated using a DLM calculation with 22 reduced frequencies. Only eleven of the calculated points have been used for the interpolation while the remaining ones serve as test points.

An example for the vertical force versus reduced frequency on a grid point near the wing root is presented in Figure 14. Very good results are achieved with the amplitude/phase interpolation.

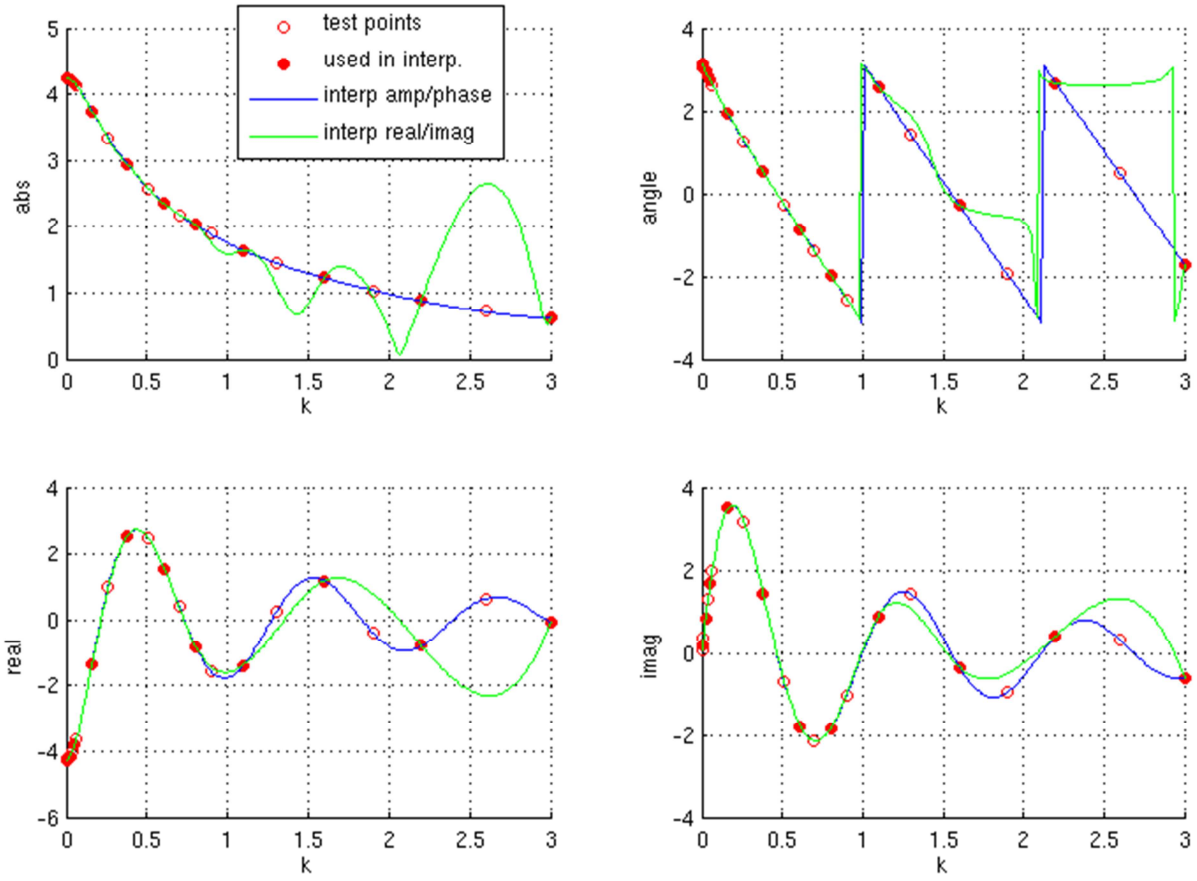

Figure 14: interpolation of grid point force Fz due to gust vs. reduced frequency

In a complete gust loads analysis, many different mass cases have to be considered. Despite the great speed-up that has been achieved by the LFD method, it is still too costly to provide CFD solutions for all of them. Therefor CFD calculations are done for a set of reference mode shapes ϕ_{gh}^{Ref} at a specific mass case only. For other mass cases, the aerodynamic data for each flexible mode is approximated by a weighted sum of the existing solutions with weight vector u_{fit}

$$Q_{g1h}^{fit} \approx Q_{g1h}^{ref} u_{fit} \tag{9}$$

where u_{fit} is calculated to minimize the squared error of an appropriately chosen target function.

Using the DLM model, three different matching algorithms to determine the weighting factors u_{fit} have been investigated during the course of the project, namely matching of structural deflections ϕ_{gh}

$$u_{fit}^{h} = \phi_{gh}^{Ref} \backslash \phi_{gh} \tag{10}$$

local panel angle of attack (downwash) w_{jh}

$$u_{fit}^{w} = w_{jh}^{Ref} \backslash w_{jh} \tag{11}$$

and pressure coefficient

$$u_{fit}^{cp} = Q_{jh}^{Ref} \backslash Q_{jh} \text{ with } Q_{jh} = Q_{jj} w_{jh} \tag{12}$$

where the latter serves as a measure on how good a match could theoretically be achieved with the selected modal basis.

Figure 15 shows results for a randomly selected test case. The wing bending moment due to mode 7 approximated with the described methods is compared to the exact solution.

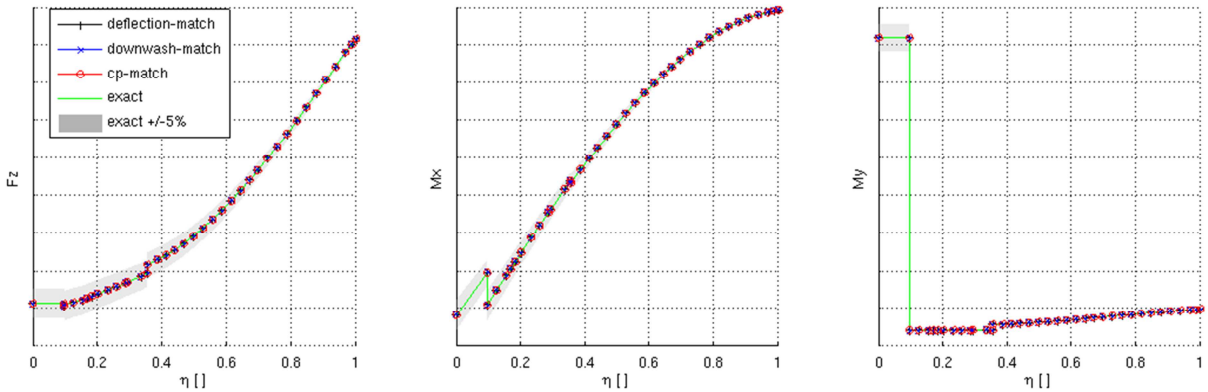

Figure 15: wing shear force, bending and torsion moment vs. span due to deflection of mode 7

In Figure 16 the generalized aerodynamic forces Q_{hh} calculated with the three different methods are shown in comparison with the exact solution. For the lowest flexible eigenmode, the three methods are virtually identical. For the given example, where a total of 90 modes have been used, differences become visible for higher modes numbers starting at about mode number 75. $Q_{hh}(82,82)$ is shown as an example.

The results for a gust loads calculations showed virtually no difference between the three different methods. For the sake of simplicity, method one was finally implemented.

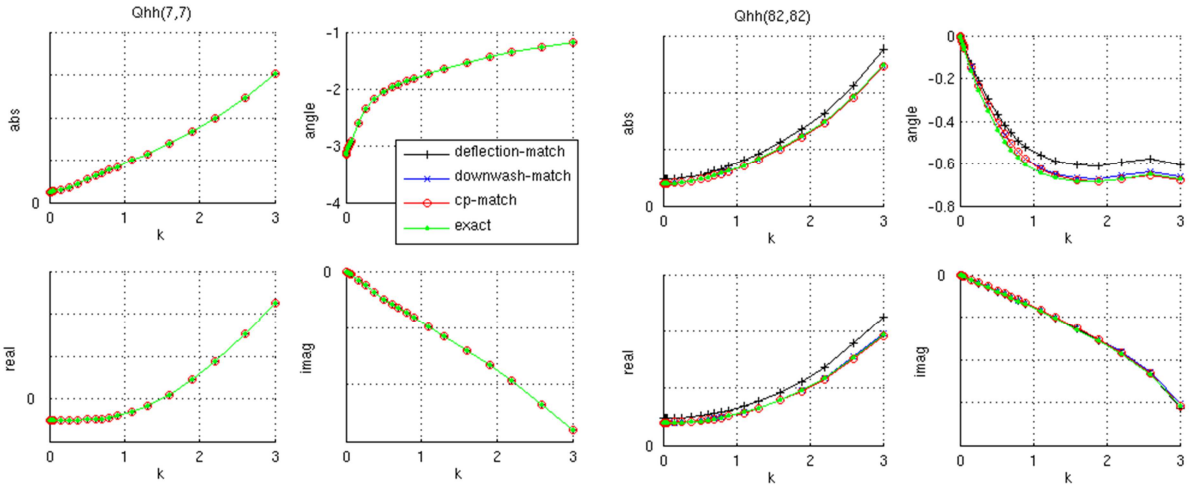

Figure 16: generalized aerodynamic forces vs. reduced frequency, exact calculation and approximations

6. GUST SIMULATIONS

The two major tasks which need to be addressed for a complete loads computation are the analysis of the continuous turbulence problem and the discrete tuned gust.

A Mach number of 0.5 at sea level was selected as flight point for this comparison which included 100 mass cases. CFD solutions were available for 90 mode shapes and 20 reduced frequencies.

Results for the incremental gust loads envelope on the wing due to continuous turbulence are presented in Figure 17. The loads levels for both methods over almost the entire wing span are very close. Notable, but still small differences are just visible for shear force and torsion moment near the wing root. These can be attributed to the discrepancies that were already evident in the rigid force gradients (Figure 5), where the simple scaling of the DLM model did not quite replicate the CFD target.

The same conclusions can be drawn for the case of the discrete tuned gust, where gust gradients ranging from 30ft to 350ft have been considered. Envelope results are shown in Figure 18.

Not only the envelopes but also the time histories agree very well, as can be seen in Figure 19, where wing root shear force and bending moment, wing tip load factor as well as aircraft angle of attack and load factor at the center of gravity are plotted for a 150ft gust.

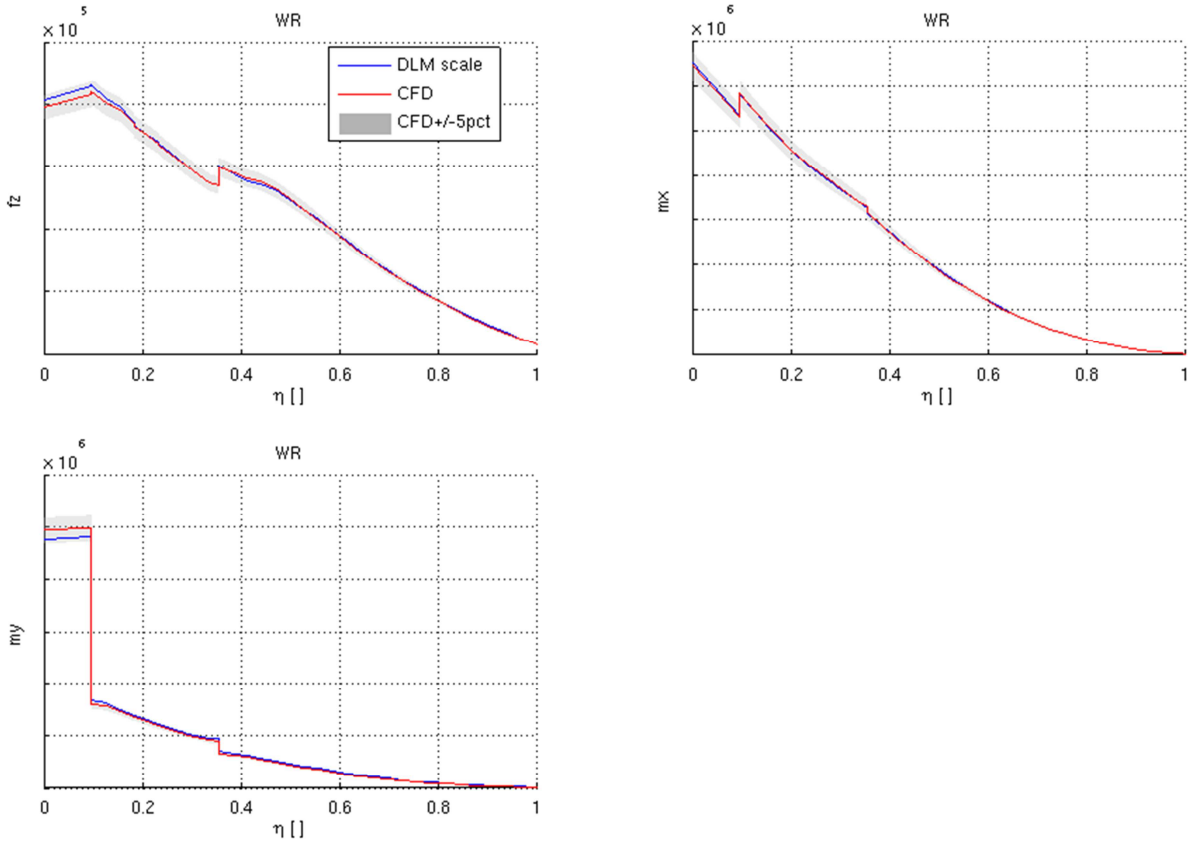

Figure 17: continuous turbulence, wing shear force, bending and torsion moment vs. span, envelope of 100 cases

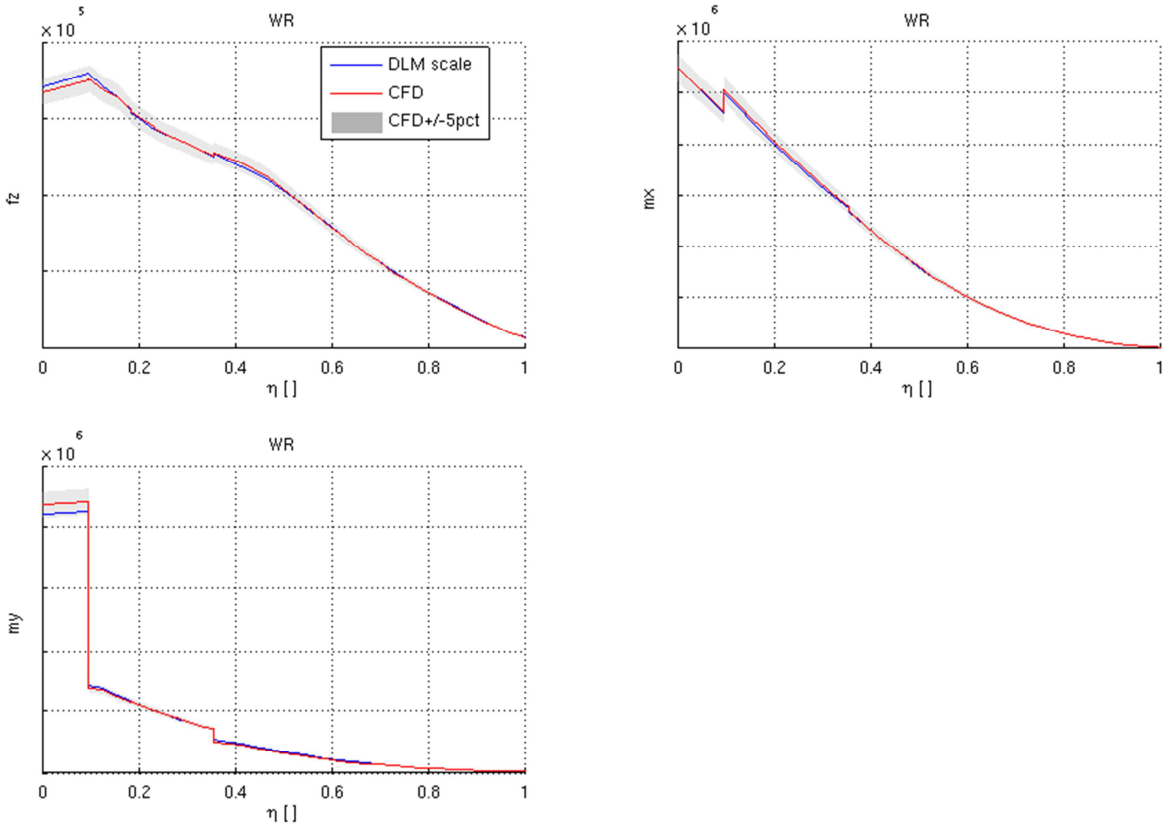

Figure 18: discrete tuned gust, wing shear force, bending and torsion moment vs. span, envelope of 100 cases

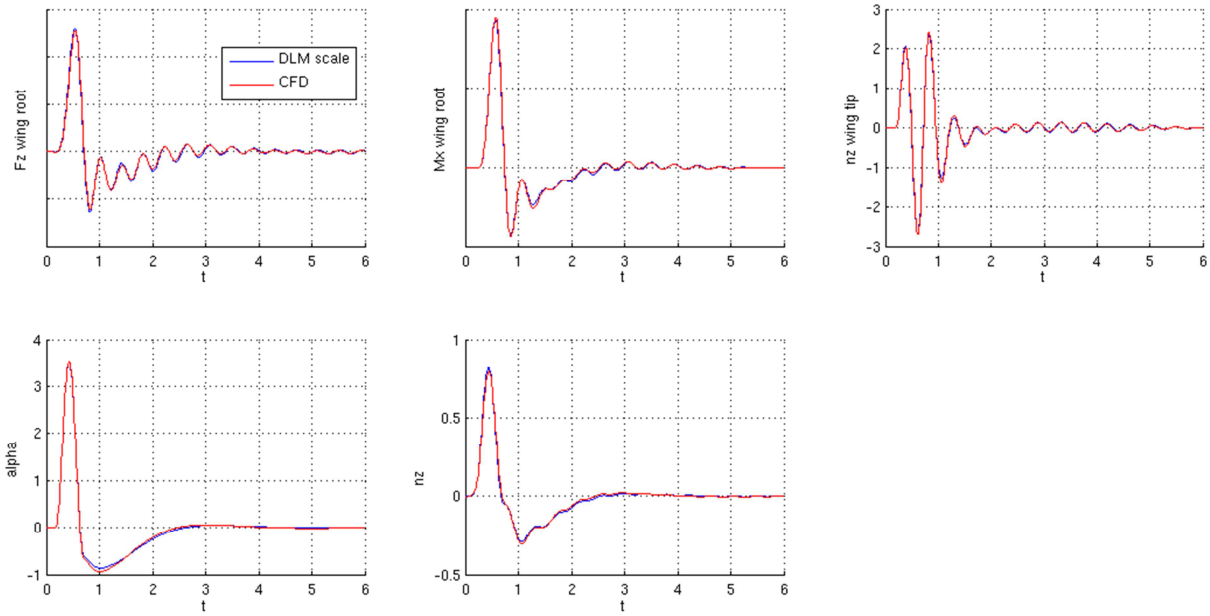

Figure 19: time history of 150ft discrete gust, scaled DLM vs. CFD based solution

7. CONCLUSIONS

This work has shown that linearized frequency domain CFD solutions provide an alternative option to well-known panel methods in the industrial context of gust loads analysis. The quality of results has been proven, in particular the important consistency between gust aerodynamics & AC rigid body motion and the quality of results of the fully frequency range

of analysis. By the change of aerodynamic input format additional requirements on interpolation and mode mapping occur, these can be however overcome by well understood processes.
This linear CFD based process will be a very good starting point to derive design loads level in gust loads analysis in the future and will minimize adjustment needs or even make them obsolete.

REFERENCES

[1] Thormann, R. and Widhalm, M. (2013). Linear-frequency-domain predictions of dynamic-response data for viscous transonic flows. AIAA-Journal.

[2] Kaiser, C., Thormann, R., Dimitrov, D., and Nitzsche, J. (2015).Time-linearized analysis of motion induced and gust-induced airloads with the DLR-Tau code. Deutscher Luft- und Raumfahrtkongress.

[3] Heinrich, R., Michler, A. (2009). Unsteady simulation of the encounter of a transport aircraft with a generic gust by CFD flight mechanics coupling, CEAS conference, Manchester UK

[4] Gerhold, T. and Galle, M. (1997). Calculation of complex three-dimensional configurations employing the DLR TAU-code. AIAA Paper 97-0167.

[5] Stickan, B., Dillinger, J., and Schewe, G. (2014). Computational aeroelastic investigation of a transonic limit-cycle-oscillation experiment at a transport aircraft wing model. Journal of Fluids and Structures, 49(0):223 – 241.

[6] Ritter, M (2012). Static and Forced Motion Aeroelastic Simulations of the HIRENSAD Wind Tunnel Model , Conference: AIAA 2012 - 53rd Structures, Structural Dynamics and Materials Conferences (SDM)

[7] Bekemeyer, P., Thormann, R., and Timme, S. (2016). Linearised Frequency Domain Gust Analysis of Large Civil Aircraft, ECCOMAS 2016

COPYRIGHT STATEMENT